Quasiparticle excitation energies for the F-center defect in LiCl

Michael P. Surh
Lawrence Livermore National Laboratory, University of California, Livermore, California 94551

Hélio Chacham
Departamento de Física, Instituto de Ciências Exatas, Universidade Federal de Minas Gerais, Caixa Postal 702, 30161 Belo Horizonte, Brazil

Steven G. Louie
Department of Physics, University of California, Berkeley, California 94720
and Materials Science Division, Lawrence Berkeley Laboratory, Berkeley, California 94720
(Received 4 November 1994)

The electronic excitation energies of an F-center defect in a LiCl crystal are calculated in the GW quasiparticle approximation. The halogen vacancy constituting the F-center is modeled in a supercell geometry that includes equilibrium lattice relaxation corrections to the defect energies. The dynamically screened Coulomb interaction, used in constructing the quasiparticle self-energy, is taken in the generalized plasmon-pole approximation using a model for the static dielectric screening. Excitations from the bound $1s$ state to conduction band critical points at X, L, and along Λ are calculated to have energies of 5.7, 4.5, and 5.0 eV, respectively, compared to experimental absorption peaks at 5.8, 4.5, and 5.0 eV. The lowest energy, intradefect level excitation shows the effect of an electron-hole interaction that is not explicitly included in the single-particle GW self-energy. This contribution is approximated, yielding a calculated energy for the fundamental absorption band of 3.4 eV, as compared to experimental observations of 3.1–3.3 eV.

I. INTRODUCTION

Halogen vacancies, known as F centers for the visible coloration they induce,[1] can be deliberately introduced into alkali halide crystals in high concentration by x-ray irradiation or by heating in an alkali-metal vapor. (Subsequent electronic transitions between the defect-induced electronic levels then yield absorption of visible light in the otherwise colorless salt.) These vacancies are considered to be prototypical point defect systems, as they are particularly simple both electronically and structurally.

F centers have been studied experimentally in many alkali halides, using techniques such as optical and transient optical absorption,[2–6] the Stark effect,[7–12] Raman spectroscopy,[13,14] and luminescence.[15] For example, optical measurements in LiCl show a fundamental absorption band centered around 3.1–3.3 eV.[2–5]

The neutral vacancy is known to contain a single bound electron and the fundamental optical absorption band arises from an electronic transition between the lowest bound levels (corresponding to $1s$ and $2p$ states). Since the electronic ground state of the defect is singly degenerate (of s-wave symmetry), there are no Jahn-Teller lattice distortions to consider. The only atomic relaxation at the vacancy consists of radial movements of the neighboring shells of atoms in towards or out from the defect. The lattice distortion will be assumed to be fixed during electronic transitions in the Franck-Condon approximation,[16] which greatly simplifies the analysis of lattice contributions to the electronic excitations.

Defect states in wide gap materials cannot be analyzed within the the effective mass approximation. The large band gaps, high effective masses, and small dielectric constants of typical alkali halides yield highly localized states for which this approach is inappropriate. Instead, F-center models typically assume an electron localized by a deep potential well (as reflected in the Mollwo-Ivey relation).[17] Fortunately, the highly localized defect states are well suited to *ab initio* cluster or supercell numerical calculations. The $1s$ electronic wave function is localized to within one or two lattice constants (see Fig. 1), while the associated structural relaxation is small and mostly confined to nearest-neighbor alkali-metal atoms.[18,19] Thus it is possible to simulate a defect in a cluster or supercell with only a few shells of neighboring atoms.

Numerous empirical and *ab initio* studies[19–25] have been made for the F-center electronic energy levels and wave functions. Independent-particle calculations are of limited accuracy, as local density approximation (LDA) calculations underestimate the 9.4 eV (Ref. 26) LiCl direct band gap by 30%,[27] while Hartree-Fock overestimates it by 80%.[28] However, GW calculations[27] and Hartree-Fock plus correlation-correction calculations[28] have obtained accurate band gaps for bulk materials. Both methods eliminate self-interaction effects[29,30] and include many-body effects on excitation energies.

This paper presents the results of pseudopotential GW and LDA calculations of the LiCl F-center levels. Elec-

0163-1829/95/51(12)/7464(7)/$06.00

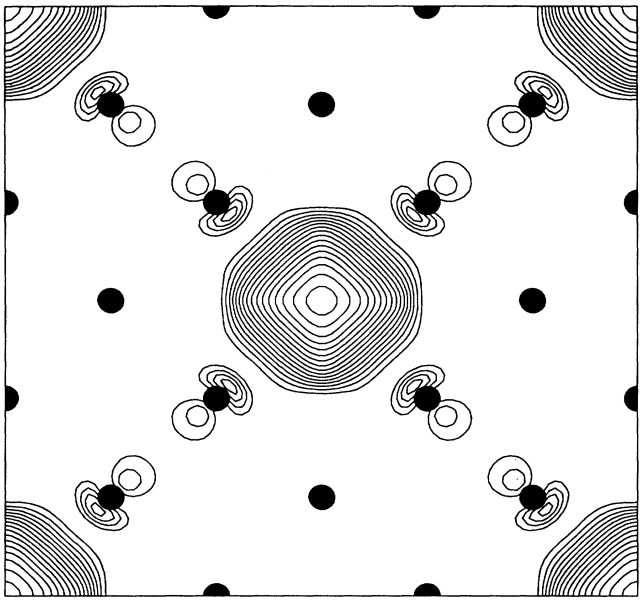

FIG. 1. Contour plot of the LiCl F-center defect $1s$ level in the (100) plane for an unrelaxed 54-atom supercell. Chlorine atoms are depicted with solid circles and lithium atoms are not shown. The peak in $|\Psi|^2$ is centered on the vacancy site, while the contours mark the density in intervals of 6% of this maximum.

tronic excitation energies related to optical absorption processes are calculated and compared to experiment. The results agree to within 0.2–0.3 eV for both single-particle and two-particle excitations.

The GW quasiparticle method treats excitations corresponding to the addition or removal of a single electron. It yields energies of single-particle-like excitations in the absence of interaction with other such excitations; for example, it correctly gives the bulk band gap energy corresponding to the creation of an infinitely separated electron-hole pair. In contrast to the energy to add or remove an electron, the F-center $1s \rightarrow 2p$ bound-state to bound-state transition energy is a two-particle property for which the electron-hole interaction is expected to enter. Here the $2p$ electron and $1s$ hole are both localized to the vicinity of the defect. This interaction is not considered in the GW approach; accordingly, a two-body correction has been estimated for the $1s \rightarrow 2p$ excitation energy.

This scheme greatly improves the excitation spectrum over that obtained using the LDA Kohn-Sham eigenvalues. Most importantly, the GW method is known to provide highly accurate band gaps. This will have a significant impact on the energies of bound states within the gap, since the LDA underestimates the band gap by 30% (therefore, a similar level of correction may be expected in the defect levels). The full exchange operator is evaluated in the GW approach, so the LDA self-interaction problem for localized states is avoided.[29]

Two-body corrections are not pertinent to the bulk band structure of the solid; rather, bulk excitations (measured in experiments that create single-particle excitations) are accurately described by the GW method alone. For example, the bulk band gap of LiCl has been calculated to be 9.1–9.3 eV in the GW approximation[27,31] versus the experimental value of 9.4 eV (Ref. 26) and the LDA value of 6.1 eV. The results presented here are consistent with previous calculations that employ similar techniques.[31]

In principle, it is straightforward to include the full dynamical and local field effects of the dielectric screening on the electron-hole interaction. It is known that these effects are important to the self-energy and band structure of LiCl (Ref. 27) and it is expected that they similarly contribute to the detailed electron-hole interaction. However, it is found that an extensive many-body treatment of the electron-hole interaction is not necessary for estimating the $1s \rightarrow 2p$ excitation energy. This bound state excitation energy is found to be 3.4 ± 0.5 eV using the GW quasiparticle energies and approximate two-body corrections. The final result is in adequate agreement with the experimental measurements of 3.1–3.3 eV.[2–5]

II. THEORETICAL METHODS

A. LDA numerical procedure

The F center is studied in the two smallest possible supercells that are consistent with a chlorine vacancy surrounded by one or more shells of chlorine atoms. Both LDA and GW calculations are performed in a supercell composed of $2\times2\times2$ primitive cells of the rocksalt structure, containing one chlorine vacancy. The self-consistent charge density is obtained with states at 8 $\vec{k}$ points in the full Brillouin zone, involving the Γ, X, and L points. The LDA calculation is also repeated for a single vacancy contained in a supercell of $3\times3\times3$ primitive rocksalt cells. The relaxation of the six lithium atoms nearest the vacancy is included in this case. Only one $\vec{k}$ point is used for the self-consistent charge density for this supercell. However, after reaching self-consistency, LDA eigenvalues are calculated at the Γ, X, and L points in order to extrapolate the dispersion of the defect bands in the 27-cell (54 atoms including the vacancy) case to the isolated defect limit.

The computational expense of the LDA calculation is minimized by employing a mixed basis approach.[34] A well-converged pseudopotential bulk band structure for LiCl requires in excess of 400 plane waves; this scales to more than 10 000 in the largest supercell considered here. The basis size may be reduced somewhat by the use of soft pseudopotentials.[35] However, a mixed basis permits an even greater reduction. In this approach, a minimal basis of local orbitals is added to the set of plane waves. The local orbitals are taken to be the numerical solutions for atomic orbitals, except that they are partially orthogonalized to the plane wave basis. They are also truncated at a finite radius to avoid the need for multicenter integrals. This local basis plus a small plane wave set is sufficient to give good valence bands and ground state charge densities.

Unfortunately, the introduction of a local basis component does not benefit the *GW* calculations as much as the LDA. The inclusion of valence atomic orbitals allows a substantial reduction in the basis size required to give the valence wave functions and the self-consistent charge density, but it does not improve the convergence rate for excited states as much. Conduction bands up to energies of 100 eV are included in the self-energy operator and so the reduced basis size is obtained at the expense of a slight reduction in the accuracy of the self-energy.

For reference, the basis set includes all plane waves with kinetic energy less than 12 Ry and chlorine $3s$ and $3p$ orbitals. This gives a fully converged (to better than 0.1 eV) bulk band gap in both the LDA and *GW*.

B. The electron-hole interaction

The $1s \rightarrow 2p$ transition of the bound electron is the most prominent feature of the optical absorption spectrum of the F center.[3,5] The resulting $2p$ electron and $1s$ hole are localized in the defect region and interact strongly. As a direct result, the LDA eigenfunctions and eigenvalues obtained from the ground state calculation do not relate to the neutral excited state. Similarly, the *GW* quasiparticle energies do not give the $1s \rightarrow 2p$ excitation energy. An accurate calculation requires inclusion of the additional electron-hole interaction.

The F-center quasiparticle excitations relate to the process of adding a quasielectron (thus taking the neutral F^0 center to a charged F^-) or creating a $1s$ quasihole (taking F^0 to F^+). Therefore, the difference between the $1s$ hole and $2p$ electron energies actually corresponds to the process of removing the $1s$ electron from one defect site and placing it in the $2p$ state on another defect site at infinite distance from the first. In that case, the single-particle wave functions should correspond reasonably well to the LDA eigenfunctions and the energies of these quasiparticle excitations can be estimated from the *GW* correction.

Although the quasiparticle energies do not directly yield the $1s \rightarrow 2p$ neutral excitation energy, it is possible to use these energies and wave functions to calculate the excitation by explicitly including the interaction between the electron and hole. This correction to the energy can be treated naturally with the two-particle Green function.[36] It gives the wave function relaxation and energy reduction that is obtained if the electron and hole are put on the same vacancy site.

In evaluating this correction, we use a model in which the exchange term and the screened Coulomb term are calculated between the $1s$ and lowest $2p$ states at the L point (the center of the defect band) for both the $2\times2\times2$ and $3\times3\times3$ supercells. The dielectric screening for the Coulomb attraction is included using static screening and neglecting local fields [i.e., macroscopic screening with $\epsilon_\infty = 2.7$ (Ref. 37)]. The dynamical screening effects on electron-hole binding and wave function are expected to be small because of the large LiCl band gap. The importance of local field effects are not examined. Only a first-order correction is considered; the $1s$ and $2p$ orbital relaxation is neglected.

C. *GW* numerical procedure

The *GW* approximation begins with the formal expression for the quasiparticle excitation energies of a system of interacting electrons in a periodic potential. The energies are solutions to[27]

$$E^{qp}\Psi^{qp}(\vec{r}) = [\hat{T} + V_{ext}(\vec{r}) + V_C(\vec{r})]\Psi^{qp}(\vec{r}) + \int d\vec{r'}\,\Sigma(\vec{r},\vec{r'};E^{qp})\Psi^{qp}(\vec{r'}) \ , \tag{2.1}$$

where $\hat{T}$ is the kinetic-energy operator, V_C is the Coulomb potential, V_{ext} is the ionic potential, and the self-energy operator Σ includes the effects of exchange and correlation. The *GW* approximation corresponds to a lowest-order expansion of the self-energy in powers of the dynamically screened Coulomb interaction W and in the energy-dependent Green function G:

$$\Sigma(\vec{r},\vec{r'};E) = i\int \frac{dE'}{2\pi} e^{-i\delta E'} G(\vec{r},\vec{r'};E-E')W(\vec{r},\vec{r'};E') \ . \tag{2.2}$$

Vertex corrections are not included in this approximation.

In this analysis, the quasiparticle approximation is made for the one-particle Green function, i.e., the electronic excitations are considered to have infinite lifetimes. It is also assumed that the LDA eigenfunctions give a good description of the quasiparticle wave functions.[27] Thus the Green function becomes

$$G(E) = \sum_{n,\vec{k}} \frac{|n\vec{k}\rangle\langle n\vec{k}|}{E - E^{qp}_{n\vec{k}} - i\eta} \tag{2.3}$$

with $|n\vec{k}\rangle$ the LDA eigenfunctions, E^{qp} the self-consistent quasiparticle energies, and η a negative infinitesimal for energies above the Fermi energy and a positive infinitesimal below. Ultimately, the exchange-correlation contribution to the LDA eigenvalue is simply replaced by the expectation of the self-energy operator to yield the quasiparticle excitation energy

$$E^{qp}_{n\vec{k}} = E^{LDA}_{n\vec{k}} + \langle n\vec{k}|\Sigma(E^{qp}_{n\vec{k}})|n\vec{k}\rangle - \langle n\vec{k}|V^{LDA}|n\vec{k}\rangle \ . \tag{2.4}$$

In practice, accurate Green functions require the inclusion of virtual intermediate states with energies as high as 100 eV. This applies to calculations of the bulk band structure[27] as well as to the defect excitations; it translates to approximately 100 bands per primitive cell. Calculations that use a minimal basis set may not include enough virtual intermediate states to adequately converge the results.

The screened Coulomb interaction in Eq. (2.2) is given by

$$W(\vec{r}_1,\vec{r}_2;\omega) = \int d\vec{r}_3 \epsilon^{-1}(\vec{r}_1,\vec{r}_3;\omega)v(\vec{r}_3,\vec{r}_2) \tag{2.5}$$

with v the bare Coulomb interaction and ϵ^{-1} the dynamic

dielectric response. Equation (2.5) is evaluated approximately since obtaining the exact quantity is impractical: the dynamical screening is computed in terms of a model static dielectric matrix expressed in a plane wave basis and a plasmon-pole model fit to two sum rules.[38] The macroscopic dielectric constant for bulk LiCl is the only input parameter (ϵ_∞=2.7).[37]

The model static dielectric matrix uses the *total* charge density from the ground state defect calculation; in this case, the defect-state electron density is included. Strictly speaking, the defect electron will not participate in screening itself so that it might be best to use the charge density of only the bulk electrons in the model. However, the change in screening upon including the defect-state electron density should be relatively small, so the full charge density is used in the model.

A bulk LiCl calculation requires 64 $\vec{k}$ points in the full Brillouin zone to adequately converge the band edges for both the LDA and *GW* calculations. Therefore, the 2×2×2 supercell employs 8-$\vec{k}$-point sampling to ensure comparable accuracy in the (bulk) band edges. It is important to recognize that the LDA calculation yields a Bloch form and a finite bandwidth for the defect-bound electrons (due to the periodic repetition of the defect in the supercell geometry). Thus the self-consistent occupation of the half-filled defect band generates a Fermi surface. This does not accurately reflect the isolated defect limit and so the occupations are constrained by placing one electron in a localized (Wannier-like) 1*s* defect orbital. The constraint alters the self-consistent charge density, although, in practice the LDA eigenvalues change by less than 0.1 eV between the two cases.

A similar modification to the Green function of Ref. 27 is critical for treating the defect state correctly. The exchange expectation of localized defect electrons should not be computed from itinerant defect states with a Fermi surface in the occupation. Thus, when constructing the Green function Eq. (2.3), the LDA Bloch wave functions for the defect band are replaced with localized states consisting of Wannier orbitals and the occupations are constrained. (The bulk band states remain in Bloch form appropriate to itinerant electrons.)

The localized defect orbital for a 1*s* orbital at site R_i is constructed from the Bloch states at Γ, *X*, and *L*

$$\Psi_i(\vec{r}) = \frac{1}{\sqrt{N}} \sum_{\vec{k}} e^{-i\vec{k}\cdot\vec{R}_i} \Psi_{\vec{k}}(\vec{r}) \qquad (2.6)$$

for $N = 8$ $\vec{k}$ points in the Brillouin zone of the 2×2×2 supercell. The energy of the localized orbital is taken to be at the center of the defect band.

There is a further complication to the Green function — each localized defect electron must be taken to have a definite spin. This is required to ensure that the self-exchange of the bound electron precisely cancels the Hartree self-interaction. The LDA Wannier orbitals from neighboring defects overlap somewhat because of the proximity of the 8 vacancy sites. Therefore, the 1*s* states at neighboring vacancies are taken to be in a paramagnetic configuration in the Green function (i.e., in a superposition of equal amounts spin up and down). This is not a critical issue; the exchange between adjacent defect states is small.

In principle, fixing the spin configuration of the defect Wannier orbital induces exchange splittings in the bulk quasiparticle local density of states.[39] This splitting is explicitly not considered, as the defect energies are not expected to be greatly affected by the spin response of the bulk electrons.

It is useful to note at this point that the LDA calculations do not include a self-interaction correction.[29] Therefore, the *GW* calculation (which has no self-interaction) will modify the 1*s* quasiparticle wave function as well as the energy. The opening of the bulk band gap in passing from the LDA to *GW* (Ref. 40) will further alter the defect wave functions. These wave function changes (which we expect to be small) have not been considered.

III. RESULTS

A. LDA results

The LDA energies for the bulk band edges and defect levels are displayed in Table I. The bulk band edges (valence band maximum and minimum, and conduction band minimum) occur at the Γ point while the defect levels correspond to the Wannier orbitals generated from 8 $\vec{k}$ points in the 2×2×2 or 3×3×3 supercells.

The top of the valence band is taken as the reference point for each of the LDA band structures. This is reasonable, as the gross features of the valence band are little affected by the presence or absence of a vacancy. The valence bandwidth is 13.16 eV in the bulk, 13.03 eV in the 8-cell defect case, and 13.13 eV in the 27 cell defect calculations.

In contrast, the band gap changes noticeably for the defect calculations. The direct band gap at Γ is found to be 6.06 eV in the bulk, comparable to that obtained from a fully converged, all-plane-wave basis calculation. The 8-cell plus vacancy calculation yields a gap of 6.33 eV and the 27-cell defect calculations a gap of 6.25–6.26 eV. This clearly shows that the supercell band gap is widened by the introduction of defect states to the gap; the effect decreases with increasing supercell size as the system approaches the bulk limit.

Finite size effects on the defect levels are also very prominent; the *F*-center 1*s* band is 1.4 eV wide in the 8-cell case and 0.3 eV wide in the 27-cell case. A nearest-neighbor tight-binding interaction describes the dispersion well; the 1*s* state at the *L* point lies at the center of the band.

It is necessary to locate the excited defect states (e.g., the 2*p* level) in order to calculate the energy of the *F*-center absorption band. Unfortunately, they are not easy to identify in the LDA. Due to the LDA band gap underestimation, no excited defect states are found to lie below the conduction band minimum (at Γ) in the 8- and 27-cell calculations. Instead, many of the 2*p* states in the supercell are resonances; thus it is difficult to unambiguously identify them.

TABLE I. Bulk band structure and defect levels with and without lattice relaxation (in eV). All energies are measured from the valence band maximum. Extrapolating from the 8- to the 27-cell to the bulk LDA calculations gives the finite-size corrections to be added to the 8-cell *GW* results. Note that the neutral defect $1s \rightarrow 2p$ excitation does not equal the difference in the $1s$ and $2p$ quasiparticle energies.

	GW 16 atom unrelaxed	LDA 16 atom unrelaxed	LDA 54 atom unrelaxed	LDA 54 atom relaxed	LDA bulk	*GW* bulk
Band gap	9.54	6.33	6.25	6.26	6.06	9.26
$1s$	5.27	4.79	4.70	4.83		
$2p$	10.73	7.82	7.18	7.23		
valence bandwidth	15.00	13.03	13.13	13.13	13.16	15.10

A good example of the problem can be found in the analysis of the lowest unoccupied state at the L point for the 2×2×2 supercell. The state has L_2' symmetry, appropriate to a tight-binding p band. This suggests an F-center-derived $2p$ excited state, but symmetry does not uniquely identify the state. The bulk conduction band edge should also have L_2' symmetry and, in fact, both of the lowest unoccupied bands at L have this symmetry. (The next highest band of L_2' symmetry lies 1 eV higher than either of these and is not a reasonable candidate for the $2p$ defect orbital.)

The LDA band gap at L for this supercell size should increase by approximately 0.1–0.2 eV from the bulk value (i.e., by the same amount as the minimum band gap, which is unambiguously determined).[41] This coincides with the energy of the higher band. Additional evidence can be gleaned from plots of the density distribution of the states; this confirms the lowest unoccupied band at L as a $2p$ defect level. The other $2p$ defect states at L are of L_3' symmetry; they are found to be resonances at higher energy that hybridize with bulk bands.

The entire $2p$ defect band is found to be 2.9 eV wide in the 8-cell case. The center of the band lies some 1.5 eV above the LDA bulk conduction band minimum, comparable to the center of the $2p$ complex at the L point. In the 27-cell case, the $2p$ bandwidth is reduced to 1.2 eV, while the center falls by 0.5–0.6 eV (see Table I).

As discussed earlier, the $2p$ levels obtained from the LDA ground state calculation are not appropriate for the neutral excited state calculation. It is interesting to first examine a LDA treatment of the excited state rather than to simply approximate the formal electron-hole correction (as will be done for the *GW* calculation). After the F electron is moved to the L_2' $2p$ state, the self-consistent LDA Wannier $2p$ level falls by 0.3 eV. The splitting of the $2p$ states at L does not change. Thus the LDA $1s \rightarrow 2p$ excitation energy with full electronic relaxation is 2.0 eV. A LDA transition state calculation[42] yields an excitation energy of 2.4 eV. This places the $2p$ level in the LDA conduction band continuum.

It is expected that the lattice relaxes slightly around the vacancy while preserving the point-group symmetry of the defect (O_h) in the ground state.[19] The 3×3×3 supercell LDA calculations indicate that the lithium atoms move outward by approximately 1% of the distance to the vacancy. This relaxation is found to lower the total energy by parts in 10^6 while raising the $1s$ state by 0.13 eV and the $2p$ state by 0.05 eV. This result is in reasonable agreement with earlier work; the calculation of Ref. 19 relaxes the two nearest-neighbor shells and obtains a similar lithium displacement and level shifts of +0.24 eV for the $1s$ state and +0.14 eV for the $2p$ state.

B. *GW* results

The *GW* results for the bulk and 2×2×2 supercell calculations are displayed in Table I. They are presented together with the LDA results because the energies must be extrapolated to the infinite supercell limit. The corrected values are presented in Table II.

Finite-size and lattice relaxation corrections to the *GW* results are obtained by comparing the different LDA calculations in Table I. For example, the $1s$ defect level does not shift relative to the valence band minimum between the unrelaxed 8- and 27-cell LDA calculations. This implies that the $1s$ energy obtained from the 8-cell *GW* calculation is well converged with respect to supercell finite-size effects. A final correction to the $1s$ level arises from the lattice relaxation at the vacancy; this is calculated in the LDA to raise the $1s$ level by 0.13 eV relative to the band edges.

In contrast to the localized $1s$ state, the valence and conduction band edges (i.e., the band gap) are noticeably affected by the size of the defect supercells employed. For example, the conduction band minimum lies too high in energy in the 8-cell calculation, as can be seen by comparing the LDA or the *GW* 8-cell and bulk calculations. The finite-size correction to the 8-cell conduction band

TABLE II. Bulk band gap and defect excitation energies (in the infinite supercell limit) compared to experiment (in eV). The calculations include the size-effect, lattice relaxation, spin-dependent, and electron-hole corrections discussed in the text. The final results are shown.

	LDA	*GW*	Expt.
Band gap	6.06	9.26	9.4[a]
$1s \rightarrow 2p$	2.4	3.4	3.1–3.3[b]
$1s \rightarrow L_c$	1.8	4.5	4.5[c]
$1s \rightarrow \Lambda_c$	2.2	5.0	5.0[c]
$1s \rightarrow X_c$	2.8	5.7	5.8[c]

[a]Reference 26.
[b]References 2–5.
[c]References 15, 32, and 33.

minimum is estimated to be −0.14 eV from comparing the LDA results or −0.21 eV from the *GW* results. A similar magnitude shift applies to the valence band maximum, yielding a total band gap correction of 0.27–0.28 eV (see Table I).

After applying the *GW* finite-size correction to the bulk band edges and the LDA relaxation correction to the $1s$ level, the $1s$ level lies 3.92 eV below the conduction band edge. The bulk *GW* calculation yields other low-lying conduction band critical points at the X and L points, which respectively lie 1.7 eV and 0.5 eV above the conduction band minimum at Γ. There is an additional local extremum along the Λ line which is estimated to lie 1.0 eV above the conduction band minimum, based on an extrapolation of the *GW* correction to the LDA eigenvalues. This yields excitation energies from the $1s$ level to conduction band critical points of 4.4 eV, 4.9 eV, and 5.6 eV. These values should be compared to measurements of peaks in the L-band optical absorption at 4.5 eV, 5.0 eV, and 5.8 eV (which corresponds the $1s$ level to the conduction band process).[15,32,33] If both the finite-size and lattice relaxation corrections to the $1s$ and conduction band levels are obtained from the LDA calculations, the extrapolated *GW* $1s$ state to the bulk excitation energies are 4.5, 5.0, and 5.7 eV, in good agreement with experiment (see Table II).

Estimating the $1s \rightarrow 2p$ excitation energy is a complicated procedure because several corrections to the $2p$ *GW* quasiparticle energies are required. Based on the 8-cell *GW* calculation, the $2p$ defect state is found to lie 5.46 eV above the $1s$ level. This corresponds to the energy of an F^- center with a $1s^1 2p^1$ configuration. It assumes that the $1s$ and $2p$ electrons are *not* in a parallel spin configuration. In contrast, the final state $2p$ electron from a $1s \rightarrow 2p$ transition should have the *same* spin as the inital $1s$ electron had, forming a singlet electron-hole pair. The calculated exchange interaction of the added $2p$ electron with the $1s$ electron is underestimated by $\frac{1}{2}$ relative to the spin parallel case. Therefore, the spin-parallel $2p$ quasiparticle energy should be reduced by approximately $\frac{1}{2}(1-1/\epsilon_\infty)$ times the unrelaxed $1s-2p$ bare exchange interaction (which is 0.42 eV for the 8-cell calculation). Thus the spin-dependent correction reduces the excitation energy by 0.13 eV.

The $2p$ defect state is much less localized than the $1s$ orbital, so that its energy is strongly dependent on the supercell size. The difference between the LDA $1s$ and $2p$ eigenvalues falls by 0.55 eV between the 8-cell and 27-cell calculations. The additional lattice relaxation correction reduces the $1s \rightarrow 2p$ difference further by 0.08 eV.

Finally, the $1s \rightarrow 2p$ excitation energy requires inclusion of the electron-hole interaction. This has been calculated in the simplest possible approximation; the LDA $1s$ (L_1 symmetry) and $2p$ (L_2' symmetry) bound states of the neutral F center are used for the hole and electron orbitals. The correction consists of a screened Coulomb attraction of −2.23 eV and singlet exchange interaction of +0.42 eV for the 8-cell calculation. These values are strongly affected by the finite-size confinement of the $2p$ orbital; they become −1.40 and +0.09 eV for the 27-cell case.

Combining these four corrections yields a $1s \rightarrow 2p$ excitation of 3.4±0.5 eV, in satisfactory agreement with the experimental estimates of 3.1–3.3 eV (see Table II).

IV. CONCLUSION

The *GW* quasiparticle energies of the bulk bands presented here are equivalent to those of similar calculations[31] and in good agreement with available experiment. The additional single-particle excitations associated with states induced by the F center are found to be similarly accurate. The $1s$ defect state is calculated to lie well within the bulk band gap of LiCl, at 4.0 eV below the conduction band minimum. The calculated transitions from the $1s$ state to other unbound conduction band states also agree well with experimental data[15,33] (see Table II).

Specifically, transitions from the $1s$ level to the (unbound) low-lying critical points in the conduction band are calculated to have energies equal to 4.5±0.2 eV for transitions to L and 5.7±0.2 eV to X. The transition to a local maximum along the Λ line has an energy of 5.0±0.2 eV. The energy differences from the $1s$ to these three lowest critical points correspond to observations of peaks in the so-called L-absorption bands of the LiCl F center in which the $1s$ electron is promoted to the conduction band.[15,32,33] Three absorption peaks are definitely associated with the F center: the L_1 peak at 4.5 eV, the L_2 peak at 5.0 eV, and the L_4 peak at 5.8 eV.[15] Therefore, the L_1 feature is identified as a transition from the $1s$ defect state to the lowest conduction band at L, the L_2 absorption peak is identified as the $1s \rightarrow \Lambda$ transition, and the L_4 peak is identified as the $1s \rightarrow X$ transition to the lowest conduction band.

There is only a small equilibrium lattice relaxation at the F center in LiCl. The nearest-neighbor lithium atoms move outwards some 1% of the distance from the vacancy. This relaxation shifts the defect $1s$ levels upwards by 0.13 eV and the $2p$ levels by 0.05 eV, relative to the conduction band edge. The calculation of Ref. 19 relaxes the nearest shells of lithium and chlorine atoms and yields a similar lithium displacement and a slightly larger level shift.

The bound $1s \rightarrow 2p$ intrasite excitation has been calculated with an approximate electron-hole correction; the resulting excitation energy is 3.4 ± 0.5 eV. This is in agreement with experimental results of 3.1–3.3 eV and is in marked contrast to the LDA prediction of 2.0–2.4 eV. (The large error estimate is a reflection of the approximate two-body correction as well as uncertainty in locating the $2p$ resonances in the LDA calculations.) The importance of the included excitonic corrections (1.3 eV in total) indicates the need for including the full many-body corrections from the two-particle Green function.

A quantitative analysis of F-center excitation energies clearly requires a many-body approach. Despite the large band gap typical of alkali halides, the dielectric screening is significant; previous work indicates that both the local field and the dynamical dependence of dielectric response must be included for the self-energy. This requirement likely extends to the electron-hole interaction. As

discussed, the electron-hole interaction has been treated with a simple approximation; nevertheless, the resulting excitation energy is in satisfactory agreement with experiment.

ACKNOWLEDGMENTS

This work was supported by NSF Grant No. DMR91-20269; by the Director, Office of Energy Research, Office of Basic Energy Sciences, Materials Science Division of the U.S. Department of Energy under Contract No. DE-AC03-76SF00098; and by the U.S. Department of Energy by Lawrence Livermore National Laboratory under Contract No. W-7405-Eng-48. CRAY computer time was provided by the Office of Energy Research of the Department of Energy and by the NSF at the Florida Supercomputing Center. H.C. acknowledges support from the Brazilian agencies CNPq, FAPEMIG, and FINEP.

[1] C. Kittel, *Introduction to Solid State Physics*, 5th ed. (Wiley, New York, 1976), p. 546.
[2] K. Fukuda, H. Matsumoto, and A. Okuda, J. Phys. Soc. Jpn. **14**, 969 (1959).
[3] C.J. Buchenauer and D.B. Fitchen, Phys. Rev. **167**, 846 (1968).
[4] R.K. Dawson and D. Pooley, Phys. Status Solidi **35**, 95 (1969).
[5] K. Takiyama, T. Fujita, H. Nojima, and M. Nishsi, Phys. Status Solidi B **115**, K59 (1983).
[6] I. Schneider, Solid State Commun. **23**, 17 (1977).
[7] G. Chiarotti, U.M. Grassano, G. Margaritondo, and R. Rosei, Nuovo Cimento B **64**, 159 (1969).
[8] U.M. Grassano, G. Margaritondo, and R. Rosei, Phys. Rev. B **2**, 3319 (1970).
[9] L.D. Bogan and D.B. Fitchen, Phys. Rev. B **1**, 4122 (1970).
[10] L.F. Stiles, M.P. Fontana, and D.B. Fitchen, Phys. Rev. B **2**, 2077 (1970).
[11] H. Ohkura, K. Imanaka, O. Kamada, Y. Mori, and T. Iida, J. Phys. Soc. Jpn. **42**, 1942 (1977).
[12] R.T. Harley and R.M. Macfarlane, J. Phys. C **16**, 1507 (1983).
[13] J.M. Worlock and S.P.S. Porto, Phys. Rev. Lett. **15**, 697 (1965); G. Benedek and G.F. Nardelli, Phys. Rev. **154**, 872 (1967).
[14] Y. Mori and H. Ohkura, J. Phys. Chem. Solids **51**, 663 (1990).
[15] K. Takiyama, J. Phys. Soc. Jpn. **44**, 1627 (1978).
[16] J. Franck, Trans. Faraday Soc. **21**, 536 (1925); E.U. Condon, Phys. Rev. **28**, 1182 (1926); **32**, 858 (1928).
[17] E. Mollwo, Nachr. Ges. Wiss. Göttingen, Math. Phys. Kl., Fachgruppe 2 **236**, 97 (1931); H.F. Ivey, Phys. Rev. **72**, 341 (1947).
[18] C.K. Ong and J.M. Vail, Phys. Rev. B **15**, 3898 (1977).
[19] R.F. Wood and J. Korringa, Phys. Rev. **123**, 1138 (1961).
[20] B.S. Gourary and F.J. Adrian, Solid State Phys. **10**, 127 (1960).
[21] R.F. Wood and H.W. Joy, Phys. Rev. **136**, A451 (1964).
[22] R.F. Wood and U. Öpik, Phys. Rev. **179**, 783 (1969).
[23] A.M. Stoneham and R.H. Bartram, Phys. Rev. B **2**, 3403 (1970).
[24] A.Y.S. Kung, A.B. Kunz, and J.M. Vail, Phys. Rev. B **26**, 3352 (1982).
[25] J.-i. Adachi and N. Kosugi, Bull. Chem. Soc. Jpn. **66**, 3314 (1993).
[26] G. Baldini and B. Bosacchi, Phys. Status Solidi **38**, 325 (1970); F.C. Brown, Ch. Gahwiller, H. Fujita, A.B. Kunz, W. Scheifley, and N. Carrera, Phys. Rev. B **2**, 2126 (1970).
[27] M.S. Hybertsen and S.G. Louie, Phys. Rev. Lett. **55**, 1418 (1985); Phys. Rev. B **34**, 5390 (1986).
[28] A.B. Kunz, Phys. Rev. B **26**, 2056 (1982).
[29] A. Zunger, J.P. Perdew, and G.L. Oliver, Solid State Commun. **34**, 933 (1980); J.P. Perdew and A. Zunger, Phys. Rev. B **23**, 5048 (1981).
[30] R.A. Heaton and C.C. Lin, J. Phys. C **17**, 1853 (1984).
[31] X. Zhu and S.G. Louie, Phys. Rev. B **43**, 14 142 (1991).
[32] G. Baldini and B. Bosacchi, Phys. Rev. **166**, 863 (1968).
[33] C.C. Klick, Phys. Rev. **137**, A1814 (1965).
[34] S.G. Louie, K.M. Ho, and M.L. Cohen, Phys. Rev. B **18**, 1774 (1979).
[35] N. Troullier and J.L. Martins, Solid State Commun. **74**, 613 (1990); Phys. Rev. B **43**, 1993 (1991).
[36] W. Hanke and L.J. Sham, Phys. Rev. B **12**, 4501 (1975).
[37] C. Kittel, *Introduction to Solid State Physics*, 5th ed. (Ref. 1), p. 309.
[38] M.S. Hybertsen and S.G. Louie, Phys. Rev. B **37**, 2733 (1988).
[39] J.M. Vail, J. Phys. Chem. Solids **51**, 589 (1990).
[40] B.M. Klein, W.E. Pickett, and L.L. Boyer, Phys. Rev. B **35**, 5802 (1987).
[41] The $2p$ defect levels lie well above the conduction band edge at the Γ point and they have a different (threefold degenerate) symmetry as well.
[42] J. Callaway and N.H. March, Solid State Phys. **38**, 171 (1984).